Theoretical Study of OH Adsorption on Pd$_x$Cu$_{3-x}$ (x = 0-3) Nano Clusters

Ali Arab[1],* and Fereydoon Gobal[2]

[1]Department of Chemistry, Semnan University, P.O. Box. 35131-19111, Semnan, Iran.
[2]Department of Chemistry, Sharif University of Technology, P.O. Box 11365-9516, Tehran, Iran.

(*) Corresponding author: a.arab@semnan.ac.ir

Abstract

Adsorption of OH on the Pd$_x$Cu$_{3-x}$(x=0-3) small clusters is investigated by density functional theory calculations. It is found that OH adsorbs in three possible modes including on top, bridge and hollow sites while the structures where OH bridges between two atoms are the most stable structures. The Pd-Pd, Pd-Cu and Cu-Cu equilibrium distances for most of the systems increase after OH adsorption and variations are higher for Pd-Pd equilibrium distances compared to Pd-Cu and Cu-Cu equilibrium distances. Adsorption of OH on Cu atom is more favored than on Pd atom. With increasing copper content of the nano-clusters the adsorption energy of OH drops to a minimum and increases with further increasing in copper content.

Keywords: OH adsorption, Pd-Cu nano clusters, DFT.

1. INRODUCTION

The oxygen reduction reaction (ORR) has been widely studied due to the specific importance in fuel cell technology [1-3]. However, slow kinetic of ORR in the cathodic compartment of the fuel cell causes a considerable loss in efficiency [4]. Using density functional theory (DFT) calculations it has been shown that the overpotential of oxygen reduction is proportional to proton and electron transfer to adsorbed oxygen and a volcano-shaped relationship between the rate of the cathodic reaction and the oxygen adsorption energy was observed [5]. Research efforts in the development of cathode electrocatalysts have been focused on decreasing the Pt content or replacing it with less expensive materials while maintaining high ORR activity [6]. Alloying of noble metals with other less expensive transition metals seems to be a potential way to achieve this goal [7-9]. It has been reported that Pd and Pd based alloys are suitable alternative electrocatalysts due to its lower costs and more abundance as well as high catalytic activity [10, 11].

DFT methods have been abundantly used for the study of different chemical systems [12-17]. The study of nano clusters with different compositions has become the topic of research in both physics and chemistry because of unusual physical properties such as structural, electronic and magnetic as well as practical applications in many different fields [14-17]. Theoretical study of chemical reactions on the surface of cluster is very helpful to understand the mechanism of these reactions on the nano particles and bulk materials.

In ORR, the adsorption of oxygen and some formed intermediates such as H_2O_2 and OH on the electrode surface influence the overall reaction rate [18, 19]. In our previous study we experimentally investigated the ORR on electrodeposited Pd-Cu alloys in alkaline media [20] and it was shown that Pd-Cu alloys were better electrocatalysts than Pd for ORR. In

addition, we theoretically studied the adsorption of atomic and molecular oxygen on Pd/Cu nano clusters [21] and it was shown that dissociation of molecular oxygen on nano clusters was exothermic and occurred more favorably on Pd/Cu mixed nano clusters compared to pure Pd nano-cluster. Here in, we investigate the adsorption of OH on Pd_xCu_{3-x}(x = 0-3) nano clusters by DFT calculations in order to clarify the relationship between theoretical results and experimental observations.

2. COMUTATIONAL METHODS

The B3PW91 hybrid density functional was used to determine optimized structures, adsorption energies, NBO charge distributions, vibrational frequencies of Pd-Cu nano clusters and their interaction with OH. B3PW91 hybrid functional exploits a combination of B3 exchange functional [22] and PW91 correlation functional [23, 24]. The LANL2TZ(f) basis set which consists of Wadt and Hay relativistic effective core potentials, valence triple zeta contraction functions, and an f-orbital polarization function [25-27] was used for Pd and Cu atoms while the MG3 semi-diffuse basis set (MG3S) was used for oxygen and hydrogen atoms [28]. The effectiveness of diffuse basis sets for performing hybrid density functional theory (HDFT) calculations has been investigated and confirmed by Truhlar [28]. All calculations were done using Gaussian 03 program [29].

3. RESULTS AND DISCUSSION
3.1. Structures of Pd_xCu_{3-x}(x = 0-3) Nano-Clusters

The validation of the selected method and the basis sets was investigated by calculation of ionization energies (IE), dissociation energies (D_{298}^0) and equilibrium bond lengths for simple Cu and Pd systems and their cations. Our calculated IEs of atomic Cu and Pd are 758.2 and 820.1 kJ mol^{-1} respectively

which are in agreement with the corresponding experimental values of 745.22 and 804.10 kJ mol^{-1} [30]. Also, our calculated dissociation energies for Cu_2 and Pd_2 are 178.7 and 154.1 kJ mol^{-1} respectively which are also in agreement with the corresponding experimental values of 201 and >136 kJ mol^{-1}[30]. Therefore, the selected method and basis sets are likely capable of predicting the properties of somewhat larger nano cluster containing Cu and Pd.

The structures of Pd_xCu_{3-x}(x= 0-3) nano clusters were optimized at B3PW91/LANL2TZ(f) level of theory. All calculations involved determination of vibrational frequencies for the validation of the local energy minima of each optimized structure. In order to find the most stable structure for Pd_xCu_{3-x}(x= 0-3) nano clusters we calculated the total energy of each nano cluster at several spin multiplicities. The most stable structures for Pd_3, Pd_2Cu, $PdCu_2$ and Cu_3 were obtained at the spin multiplicities of 3, 2, 1 and 2 respectively. The most stable structure of Pd_3 which obtained at spin multiplicity of 3 is in accordance with the literature [31] where it has been shown that for Pd_n(n=2-7) clusters the most stable structures occurred at spin multiplicity of 3. It should be mentioned that the most stable structure of each nano cluster has a triangular shape (Fig. 1). NBO atomic charges, equilibrium bond distances and average bond distances are collected in Table 1 for the most stable nano clusters. In this Table and other parts of this study, the letters (S), (D), (T) and (Q) behind clusters formula present the spin multiplicity of 1, 2, 3 and 4 respectively. Higher negative charge on Pd atoms is in line with expectations because of its higher electronegativity. As shown in Table 1 it seems that Pd-Pd equilibrium distance is longer than Pd-Cu and Cu-Cu equilibrium distances.

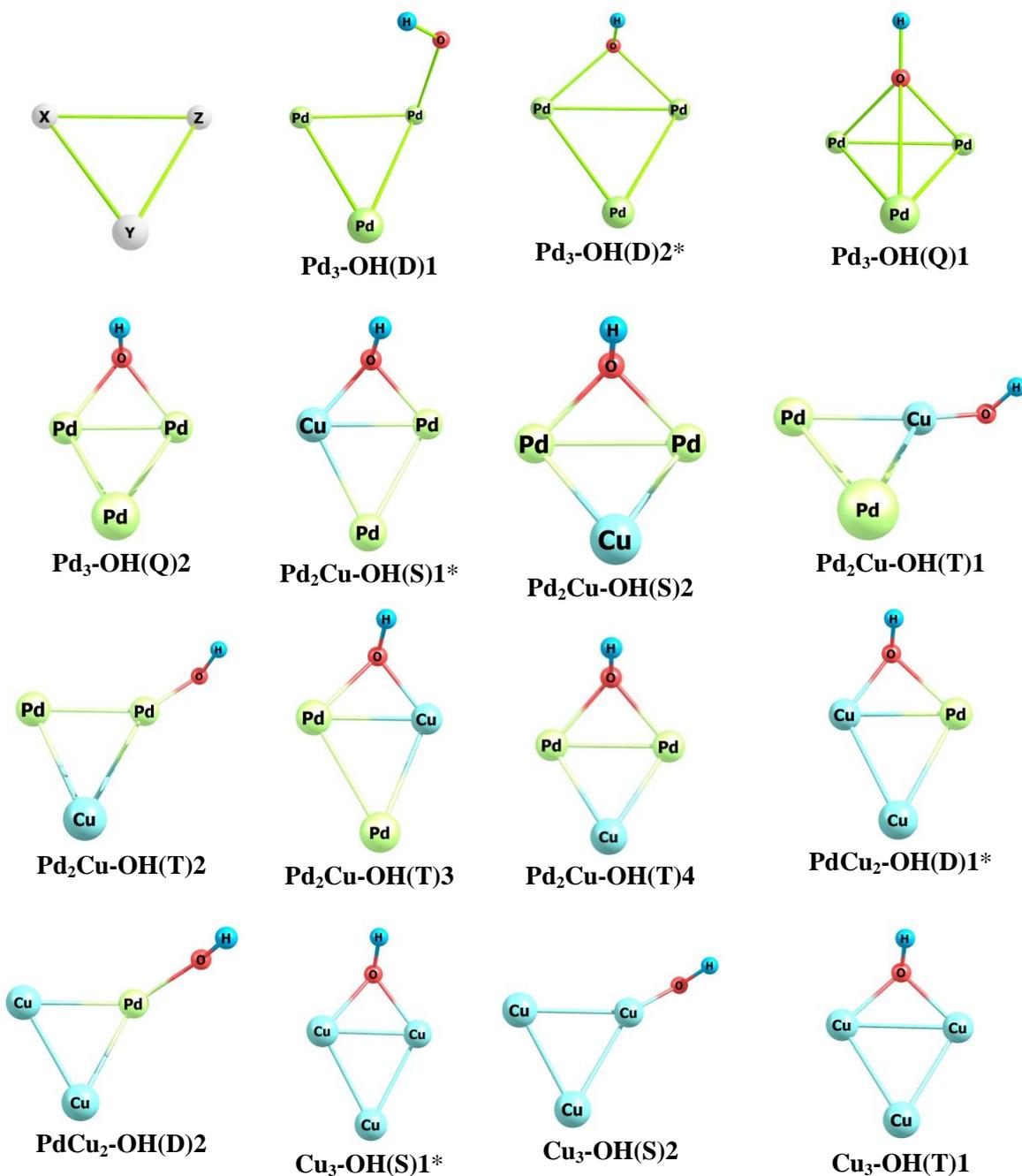### 3.2. OH Adsorption on Pd_xCu_{3-x}(x = 0-3) Nano-Clusters

The bond length of O-H, calculated at B3PW91/MG3S level of theory is 0.97 Å which is in agreement with the experimental value of 0.96 Å [30]. Moreover, the calculated vibrational frequency of OH is 3747.40 cm^{-1} while the corresponding experimental value is 3400 cm^{-1} [30]. Fig. 1 presents different adsorption modes of OH on Pd_xCu_{3-x}(x = 0-3) nano clusters. In this figure and other parts of this study, the numbers 1, 2, 3 and 4 behind cluster formula show different adsorption modes on a special nano cluster with a defined spin multiplicity and letters (S), (D), (T) and (Q) as previously mentioned signify the spin multiplicity of the system. The most stable adsorption mode for each nano cluster labeled with *. Three different modes of adsorption including on top, bridge and hollow sites have been optimized. It is observed that the most stable adsorption mode occurs when OH adsorbs on bridge site.

Table 2 presents the calculated values of adsorption energy, vibrational frequency and bond length of OH for systems of Fig. 1. The adsorption energy was calculated according to $E_{ads} = E_{cluster-OH} - (E_{cluster} + E_{OH})$ equation, where $E_{cluster-OH}$ is the total energy of cluster-OH system, $E_{cluster}$ is the total energy of cluster and E_{OH} is the total energy of OH entity. The OH bond length for all of the systems reduces (4th column of Table 2) after adsorption on the nano cluster surfaces and therefore the vibrational frequencies increase accordingly. Also, NBO charge distribution shows that the O atom attains large negative charge while the H and other nearest neighbor atoms are positively charged. Variation of total NBO charge of clusters after OH adsorption against copper percentage is shown in Fig. 2. The positive values of total NBO charge of clusters indicate that charge transfer occur significantly from clusters to the OH entity. Also with increasing copper content of clusters the total NBO charge of clusters increases from 0.53 for Pd_3 cluster to 0.76 for Cu_3 cluster. The OH adsorption energies indicate that copper atoms are preferable sites for adsorption of OH compared to the palladium atoms (2nd column of Table 2). Also, with increasing the amount of copper in nano clusters the affinity of Pd atoms reduce for OH adsorption as signified by the lower adsorption energy of Pd_2Cu -OH(T)2 system versus Pd_3 -OH(D)1 system where OH adsorbs on top of the Pd atom and OH adsorption energy reduces from -262.52 to -198.77 kJ mol^{-1}. Fig. 3 presents variation of OH adsorption energy versus copper percentage in nano cluster. In Fig. 3-a OH adsorbs on top site while in Fig. 3-b OH adsorbs on bridge site. The minimum points in these figures (around 40% copper content) show that with further increasing the amount of copper, the available Pd sites reduce and OH adsorbs directly on Cu

Table 1. *NBO atomic charges and equilibrium distances for Pd_xCu_{3-x}(x= 0-3) nano clusters.*

Nano cluster	NBO atomic charges			Equilibrium distances (Å)			Average equilibrium distances (Å)		
	X	Y	Z	X-Y	X-Z	Y-Z	Pd-Pd	Pd-Cu	Cu-Cu
Pd_3-(T)	0.069	-0.034	-0.034	2.58	2.58	2.46	2.54	---	---
Pd_2Cu-(D)	-0.032	-0.032	0.064^{Cu}	2.52	2.46	2.46	2.52	2.46	---
$PdCu_2$-(S)	-0.142^{Pd}	0.071	0.071	2.44	2.44	2.36	---	2.44	2.36
Cu_3-(D)	-0.157	0.078	0.078	2.44	2.44	2.28	---	---	2.39

Figure 1. *Different adsorption modes of OH on $Pd_xCu_{3-x}(x = 0-3)$ nano clusters. *: show the most stable structure in each system.*

atom which is energetically favorable and OH adsorption energy increases. It should be added that the maximum rate of oxygen reduction on Pd-Cu alloys was observed around 40% copper content [20].

Table 3 presents the average equilibrium distances of atoms in nano cluster after OH adsorption and nano cluster-OH distances. According to the results of Tables 3 and 1 it is clear that in Pd_3-OH system, Pd-Pd
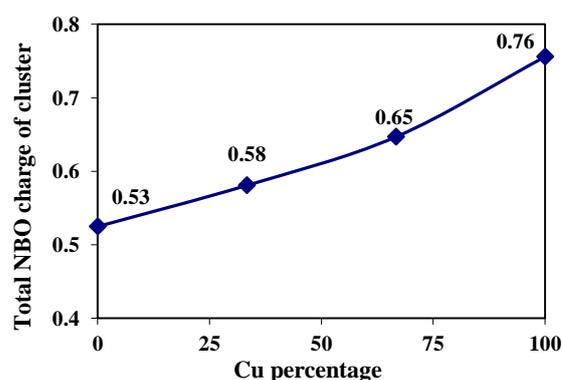
Figure 2. *Total NBO charge of clusters versus copper percentage after OH adsorption.*

equilibrium distances increase in the range of 0.05 to 0.19 Å after OH adsorption. In
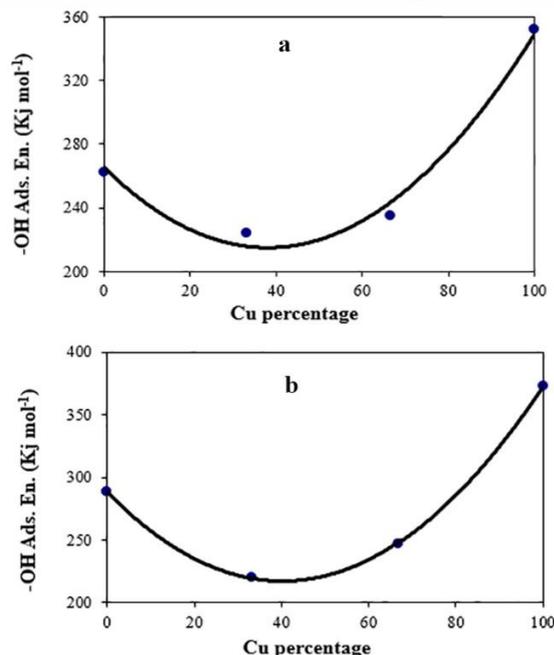
Figure 3. *Variations of OH adsorption energy versus copper percentage on top site (a) and on bridge site (b).*

Pd_2Cu-OH system, Pd-Pd equilibrium distances vary in the range of -0.01 to 0.37 Å after OH adsorption while Pd-Cu equilibrium distances increase in the range The minimum vibrational frequencies of optimized structures have been also reported in Table 3 in order to confirm that the optimized structures are real local minima.of 0.01 to 0.09 Å. In $PdCu_2$-OH system, Pd-Cu equilibrium distances vary in the range of -0.02 to 0.09 Å after OH adsorption while Cu-Cu equilibrium distances vary in the range of 0.00 to 0.07 Å. And finally in Cu_3-OH system, Cu-Cu equilibrium distances vary in the range of -0.03 to 0.09 Å. These results indicate that after OH adsorption most of the equilibrium bond distances increase and these variations are higher for Pd-Pd equilibrium distances compared to the Pd-Cu and Cu-Cu equilibrium distances. Moreover, results of Table 3 show that Cu-OH equilibrium distances are shorter compared to Pd-OH equilibrium distances which is in agreement with higher OH adsorption energy on Cu atom.

Table 2. *Adsorption energies, vibrational frequencies, OH bond length and NBO atomic charges for the systems of Fig. 1 calculated at B3PW91 level of theory.*

System	Ads. En. $(kJ\,mol^{-1})$	OH freq. (cm^{-1})	OH bond length (Å)	NBO atomic charges				
				X	Y	Z	O	H
Free OH	---	3747.66	0.972	---	---	---	-0.400	0.400
Pd_3-OH(D)1	-262.52	3802.78	0.964	0.076	0.088	0.251	-0.869	0.455
Pd_3-OH(D)2*	-288.31	3824.55	0.963	0.268	-0.011	0.268	-0.996	0.471
Pd_3-OH(Q)1	-193.97	3787.48	0.963	0.223	0.220	0.221	-1.146	0.482
Pd_3-OH(Q)2	-239.53	3818.48	0.963	0.271	-0.029	0.272	-0.980	0.466
Pd_2Cu-OH(S)1*	-252.84	3828.57	0.962	0.455^{Cu}	-0.082	0.208	-1.049	0.468
Pd_2Cu-OH(S)2	-219.75	3817.73	0.963	0.150	0.226^{Cu}	0.150	-0.992	0.466
Pd_2Cu-OH(T)1	-224.31	3868.25	0.960	0.039	0.080	0.465^{Cu}	-1.034	0.450
Pd_2Cu-OH(T)2	-198.77	3846.72	0.962	0.039	0.138^{Cu}	0.274	-0.901	0.450
Pd_2Cu-OH(T)3	-210.77	3812.11	0.964	0.259	-0.069	0.453^{Cu}	-1.104	0.461
Pd_2Cu-OH(T)4	-233.28	3825.33	0.963	0.262	0.007^{Cu}	0.262	-0.995	0.464
$PdCu_2$-OH(D)1*	-247.22	3844.75	0.961	0.414	-0.013	0.246^{Pd}	-1.107	0.460
$PdCu_2$-OH(D)2	-202.47	3871.26	0.960	0.170	0.170	0.170^{Pd}	-0.954	0.444
Cu_3-OH(S)1*	-373.01	3871.83	0.959	0.426	-0.096	0.426	-1.221	0.464
Cu_3-OH(S)2	-351.68	3876.99	0.959	0.197	0.198	0.291	-1.130	0.444
Cu_3-OH(T)1	-246.78	3833.85	0.962	0.282	0.090	0.280	-1.123	0.472

*: show the most stable structure in each system.

Table 4 presents the Mulliken atomic spin densities before and after OH adsorption on nano clusters. It seems that after OH adsorption, spin density on oxygen atom highly reduces while spin density on hydrogen atom marginally varies. Furthermore, spin densities on palladium and copper atoms almost increase after OH adsorption. NBO charge densities demonstrated (Table 2) that after OH adsorption oxygen atom attains large negative charge while the hydrogen and other nearest neighbor atoms are positively charged. Therefore it seems that spin distribution on atoms is in contrast with charge distribution and with increasing negative charge on atoms the spin density reduces.

4. CONCLUSION

In this study, adsorption of OH on Pd_xCu_{3-x}(x = 0-3) nano clusters is investigated by B3PW91 hybrid functional. It is observed that, OH adsorbs in three different modes including on top, bridge and hollow sites and most stable structures are due to the adsorption of OH on bridge sites. After OH adsorption, the bond length of OH reduces while most of the other equilibrium distances including Pd-Pd, Pd-Cu and Cu-Cu increase and these variations are higher for Pd-Pd equilibrium distances. OH adsorption energies indicate that the copper atoms are preferable sites for OH adsorption. Diagram of OH adsorption energy on Pd_xCu_{3-x}(x = 0-3) nano clusters against copper percentage shows a minimum point which corresponds to the maximum point in the rate diagram of ORR.

ACKNOWLEDGMENT

Table 3. *Average equilibrium distances (Å) of atoms after OH adsorption and average nano-cluster-OH distances (Å).*

System	Minimum Vib. Freq. (cm⁻¹)	Average cluster-OH distances (Å)		Average equilibrium distances (Å)		
		Pd-OH	Cu-OH	Pd-Pd	Pd-Cu	Cu-Cu
Pd_3-OH(D)1	45.36	1.90	---	2.59	---	---
Pd_3-OH(D)2*	67.92	2.04	---	2.73	---	---
Pd_3-OH(Q)1	70.07	2.18	---	2.69	---	---
Pd_3-OH(Q)2	90.33	2.11	---	2.59	---	---
Pd_2Cu-OH(S)1*	71.63	2.05	1.91	2.63	2.52	---
Pd_2Cu-OH(S)2	115.73	2.06	---	2.89	2.47	---
Pd_2Cu-OH(T)1	74.75	---	1.77	2.54	2.48	---
Pd_2Cu-OH(T)2	54.90	1.93	---	2.51	2.47	---
Pd_2Cu-OH(T)3	73.06	2.18	1.92	2.53	2.55	---
Pd_2Cu-OH(T)4	53.30	2.09	---	2.72	2.51	---
$PdCu_2$-OH(D)1*	65.38	2.15	1.94	---	2.53	2.37
$PdCu_2$-OH(D)2	39.11	1.95	---	---	2.48	2.36
Cu_3-OH(S)1*	88.36	---	1.97	---	---	2.38
Cu_3-OH(S)2	57.81	---	2.12	---	---	2.41
Cu_3-OH(T)1	94.25	---	1.92	---	---	2.48

Table 4. *Mulliken atomic spin densities before and after OH adsorption on nano clusters.*

System	Mulliken atomic spin density (before OH adsorption)			Mulliken atomic spin density (after OH adsorption)				
	X	Y	Z	X	Y	Z	O	H
Free OH	1.02^O	-0.02^H	---	---	---	---	---	---
Pd_3-OH(D)1	0.92	0.55	0.55	0.36	0.37	0.27	-0.01	0.01
Pd_3-OH(D)2*	0.92	0.55	0.55	0.40	0.30	0.25	0.06	-0.01
Pd_3-OH(Q)1	0.92	0.55	0.55	0.91	0.93	0.92	0.20	0.04
Pd_3-OH(Q)2	0.92	0.55	0.55	1.05	0.77	0.85	0.28	0.06
Pd_2Cu-OH(S)1*	0.49	0.51	0.00^{Cu}	---	---	---	---	---
Pd_2Cu-OH(S)2	0.49	0.51	0.00^{Cu}	---	---	---	---	---
Pd_2Cu-OH(T)1	0.49	0.51	0.00^{Cu}	0.71	0.66	0.33^{Cu}	0.30	0.00
Pd_2Cu-OH(T)2	0.49	0.51	0.00^{Cu}	0.57	0.10^{Cu}	0.97	0.36	0.00
Pd_2Cu-OH(T)3	0.49	0.51	0.00^{Cu}	0.72	1.00	0.14^{Cu}	0.12	0.01
Pd_2Cu-OH(T)4	0.49	0.51	0.00^{Cu}	0.72	0.26^{Cu}	0.72	0.29	0.00
$PdCu_2$-OH(D)1*	---	---	---	0.18	0.22	0.54^{Pd}	0.05	0.02
$PdCu_2$-OH(D)2	---	---	---	0.16	0.18	0.44^{Pd}	0.18	0.04
Cu_3-OH(S)1*	0.58	0.21	0.21	---	---	---	---	---
Cu_3-OH(S)2	0.58	0.21	0.21	---	---	---	---	---
Cu_3-OH(T)1	0.58	0.21	0.21	0.48	0.49	0.95	0.06	0.02

REFERENCES

1. Zhdanov, V.P., Kasemo, B. (2006). "Kinetics of electrochemical O_2 reduction on Pt", *Electrochem. Commun.,* 8: 1132-1136.
2. Garcia-Contreras, M.A., Fernandez-Valverde, S.M., Vargas-Garcia, J.R. (2007). "Oxygen reduction reaction on cobalt–nickel alloys prepared by mechanical alloying", *J. Alloys Compd.,* 434–435: 522-524.
3. He, W., Liu, J., Qiao, Y., Zou, Z., Zhang, X., Akins, D.L., Yang, H. (2010). "Simple preparation of Pd–Pt nanoalloy catalysts for methanol-tolerant oxygen reduction", *J. Power Sources*, 195: 1046-1050.
4. Antolini, E., Lopes, T., Gonzalez, E.R. (2008). "An overview of platinum-based catalysts as methanol-resistant oxygen reduction materials for direct methanol fuel cells", *J. Alloys Compd.*, 461: 253-262.
5. Norskov, J.K., Rossmeisl, J., Logadottir, A., Lindqvist, L., Kitchin, J.R., Bligaard, T., Jonsson, H. (2004). "Origin of the overpotential for oxygen reduction at a fuel cell cathode", *J. Phys. Chem. B*, 108: 17886-17892.
6. Markovic, N.M., Schmidt, T.J., Stamenkovic, V., Ross, P.N. (2001). "Oxygen Reduction Reaction on Pt and Pt Bimetallic Surfaces: A Selective Review", *Fuel Cells*, 1: 105-116.
7. Neergat, M., Shukla, A.K., Gandhi, K.S. (2001). "Platinum-based alloys as oxygen–reduction catalysts for solid–polymer–electrolyte direct methanol fuel cells", *J. Appl. Electrochem.*, 31: 373-378.
8. Toda, T., Igarashi, H., Uchida, H., Watanabe, M. (1999). "Enhancement of the Electroreduction of Oxygen on Pt Alloys with Fe, Ni, and Co", *J. Electrochem. Soc.*, 146: 3750-3756.
9. Li, W., Zhou, W., Li, H., Zhou, Z., Zhou, B., Sun, G., Xin, Q. (2004). "Nano-stuctured Pt–Fe/C as cathode catalyst in direct methanol fuel cell", *Electrochim. Acta*, 49: 1045-1055.
10. Fernandez, J.L., Walsh, D.A., Bard, A.J. (2005). "Thermodynamic Guidelines for the Design of Bimetallic Catalysts for Oxygen Electroreduction and Rapid Screening by Scanning Electrochemical Microscopy. M−Co (M: Pd, Ag, Au)", *J. Am. Chem. Soc.*, 127: 357-365.
11. Lima, F.H.B., Zhang, J., Shao, M.H., Sasaki, K., Vukmirovic, M.B., Ticianelli, E.A., Adzic, R.R. (2007). "Catalytic activity-d-band center correlation for the O_2 reduction reaction on platinum in alkaline solutions", *J. Phys. Chem. C*, 111: 404-410.
12. Hatami, M., Majles Ara, M.H., Rostami, A., Dolatyari, M., Mahmudi, M., Baghban, H., Rasooli, H., Afsare, M. (2012). "Lead Selenide Nanomaterials: Hydrothermal Synthesis, Characterization, Optical Properties and DFT Calculations", *Int. J. Nanosci. Nanotechnol.*, 8: 149-156.
13. Eslamifar, Z. (2014). "The Theoretical Study on a Nano Biosystem Consisting of Nano Tube-Catalytic Site of Bacillus Subtilis α-Amylase, PDB: 1UA7", *Int. J. Nanosci. Nanotechnol.*, 10: 35-44.
14. Arab, A., Gobal, F., Nahali, N., Nahali, M. (2013). "Electronic and Structural Properties of Neutral,Anionic, and Cationic Rh_xCu_{4-x} (x = 0–4) Small Clusters: A DFT Study", *J. Clust. Sci.*, 24: 273-287.
15. Mahtout, S., Tariket, Y. (2016). "Electronic and magnetic properties of $CrGe_n$ ($15 \leqslant n \leqslant 29$) clusters: A DFT study", *Chem. Phys.*, 472: 270-277.
16. Kumar, V., Shah, E.V., Roy, D.R. (2015). "DFT investigation on A_4B_4 (A=Cu, Ag; B=As, Sn) metal–semiconductor alloy clusters for potential nanomaterials", *Physica E*, 68: 224-231.

17. Francisco, H., Bertin, V., Agacino, E., Poulain, E., Castro, M. (2015). "Dissociation of N_2O promoted by Rh_6 clusters. A ZORA/DFT/PBE study", *J. Mol. Catal. A:Chem.*, 406: 238-250.

18. Stamenkovic, V., Mun, B.S., Mayrhofer, K.J.J., Ross, P.N., Markovic, N.M., Rossmeisl, J., Greeley, J., Norskov, J.K. (2006). "Changing the Activity of Electrocatalysts for Oxygen Reduction by Tuning the Surface Electronic Structure", *Angew. Chem. Int. Ed.*, 45: 2897-2901.

19. Teliska, M., Murthi, V.S., Mukerjee, S., Ramakera, D.E. (2005). "Correlation of Water Activation, Surface Properties, and Oxygen Reduction Reactivity of Supported Pt–M/C Bimetallic Electrocatalysts Using XAS ", *J. Electrochem. Soc.*, 152: A2159-A2169.

20. Gobal, F., Arab, R. (2010). "A preliminary study of the electro-catalytic reduction of oxygen on Cu–Pd alloys in alkaline solution", *J. Electroanal. Chem.*, 647: 66-73.

21. Gobal, F., Arab, R., Nahali, M. (2010). "A comparative DFT study of atomic and molecular oxygen adsorption on neutral and negatively charged Pd_xCu_{3-x} (x = 0–3) nano-clusters", *J. Mol. Struct. Theochem.*, 959: 15-21.

22. Becke, A.D. (1993). "A new mixing of Hartree–Fock and local density-functional theories", *J. Chem. Phys.*, 98: 1372-1377.

23. Predew, J.P., Chevary, J.A., Vosko, S.H., Jackson, K.A., Pederson, M.R., Singh, D.J., Fiolhais, C. (1992). "Atoms, molecules, solids, and surfaces: Applications of the generalized gradient approximation for exchange and correlation", *Phys. Rev. B.*, 46: 6671-6688.

24. Perdew, J.P., Wang, Y. (1992). "Accurate and simple analytic representation of the electron-gas correlation energy", *Phys. Rev. B*, 45: 13244-13250.

25. Hay, P.J., Wadt, W.R. (1985). "Ab initio effective core potentials for molecular calculations. Potentials for K to Au including the outermost core orbitals", *J. Chem. Phys.*, 82: 299-310.

26. Ehlers, A.W., Bohm, M., Dapprich, S., Gobbi, A., Hollwarth, A., Jonas, V., Kohler, K.F., Stegmann, R., Veldkamp, A., Frenking, G. (1993). "A set of f-polarization functions for pseudo-potential basis sets of the transition metals Sc-Cu, Y-Ag and La-Au", *Chem. Phys. Lett.*, 208:111-114.

27. Roy, L.E., Hay, P.J., Martin, R.L. (2008). "Revised Basis Sets for the LANL Effective Core Potentials", *J. Chem. Theory Comput.*, 4: 1029-1031.

28. Lynch, B.J., Zhao, Y., Truhlar, D.G. (2003). "Effectiveness of Diffuse Basis Functions for Calculating Relative Energies by Density Functional Theory", *J. Phys. Chem. A*, 107:1384-1388.

29. Frisch, M.J., et al. (2003). Gaussian 03, Revision B.03, Gaussian, Inc., Pittsburgh PA.

30. Lide, D.R. (2009). "*CRC Handbook of Chemistry and Physics*", CRC Press/Taylor and Francis, Boca Raton.

31. Bertani, V., Cavallotti, C., Masi, M., Carra, S. (2003). "A theoretical analysis of the molecular events involved in hydrocarbons reactivity on palladium clusters", *J. Mol. Catal. A: Chem.*, 204–205:771-778.